Electronic Journal of Qualitative Theory of Differential Equations
206, No. 55, 1–15; https://doi.org/10.14232/ejqtde.206.1.55 www.math.u-szeged.hu/ejqtde/

Dynamic behavior of a predator–prey model in a critical regime for predator with immigration in both species

Érika Diz-Pita ✉ [1,2] and **M. Victoria Otero-Espinar**[1,2]

[1]Departamento de Estatística, Análise Matemática e Optimización,
Universidade de Santiago de Compostela, Spain
[2]Centro de Investigación y Tecnología Matemática de Galicia, CITMAga.

Received 24 April 2026, appeared 24 October 2026
Communicated by Gabriele Villari

Abstract. Most ecological interactions occur in open ecosystems, where species can enter or leave. Predator–prey dynamics are no exception. This work generalizes a predator–prey model by incorporating immigration for both species, making it more biologically relevant. We analyze a system with a Holling type II functional response in the positive quadrant of the Poincaré disk, the biologically meaningful region, including its behavior near infinity. We identify several realizable phase portrait configurations and provide sufficient conditions for the occurrence of a Hopf bifurcation giving rise to a small-amplitude limit cycle.

Keywords: population dynamics, predator–prey, global dynamics, limit cycle, Hopf bifurcation.

2020 Mathematics Subject Classification: 34A34, 34C07, 34C60, 34C23.

1 Introduction

The field of biomathematics aims to understand and explain the evolution of biological systems at different scales. Differential equations and dynamical systems are powerful tools for this purpose, as evidenced by classic examples like Lotka–Volterra equations and the SIR model. This work focuses on predator–prey interactions, a subject of longstanding interest. While numerous studies exist, and new advances are continuously being made (see [1, 7, 9, 15, 21, 22, 24, 25]), real-world complexities demand further exploration. One such aspect that deserves further study is immigration, a ubiquitous phenomenon across all animal groups. From plankton to whales, migration significantly impacts population dynamics (see [14, 18]).

Recent studies have explored the effects of immigration on different populations using diverse modeling approaches, including delay equations [3, 5, 8, 31] and fractional order models

✉Corresponding author. Email: erikadiz.pita@usc.es

[4]. Notably, Sugie et al. [28] incorporated constant prey immigration into the Rosenzweig-MacArthur model, demonstrating its potential for coexistence and highlighting its impact on simple models. Similarly, Priyanka et al. [26] investigated non-constant, population-dependent immigration in both prey and predator populations (but not simultaneously).

Although Tahara et al. [29] analyzed predator–prey models with various functional responses and immigration representations, they lacked an analytical study of immigration in both species. Mukherjee [23] explored a three-dimensional model with constant prey immigration, but focused only on equilibria and stability.

There are also discrete-time models for predator–prey systems with immigration. However, these models consistently restrict immigration to a single species. For instance, Kangalgil et al. [19] built upon the Holling type I discrete system of Rana [27] by introducing a constant immigration rate for prey. Their analysis focused on the equilibria and the dynamical shifts caused by the immigration term, but while they explored bifurcation, their results stemmed from numerical simulations rather than direct analytical solutions.

Other works including the immigration effect can be found in [11], where different predator–prey models have been analyzed and compared.

Motivated by these gaps, in [10] we presented a comprehensive analysis of the global dynamics in a predator–prey system with Holling type I functional response and constant immigration in both populations. We built upon existing research by incorporating the new feature of immigration and analyzing dynamics beyond local behavior through compactification, similar to recent studies on classical models [12]. This approach offers valuable insights for studying real-world ecosystems with migratory prey and predators.

Although simple models are often valid for modeling certain phenomena, we aim to go a step further and present a system with a functional response closer to reality. More precisely, we consider a Holling type II functional response.

Our starting point is the general system

$$\begin{aligned} \dot{x} &= rx - \frac{ax^{1+\alpha}y}{1+hx^{1+\alpha}} + c_1, \\ \dot{y} &= \frac{bx^{1+\alpha}y}{1+hx^{1+\alpha}} - ny + c_2, \end{aligned} \tag{1.1}$$

where r represents the growth rate of prey; n is the death rate of predator; a is the rate of predation; b is the conversion rate of eaten prey into new predators; h and α are the functional response coefficients (which involve, for example, the handling time); and c_1 and c_2 are the immigration rates of prey and predator, respectively. All these real parameters are positive due to their biological meaning.

The case with $\alpha = h = 0$ has been studied in [10]. That case corresponds to a Holling type I functional response. In this paper we consider the case with $\alpha = 0$, $h \neq 0$, which corresponds to the more realistic Holling type II functional response. Due to the complexity of the system and the number of parameters, we impose an additional condition $b = hn$.

This equality is not intended to represent an empirically established relationship between the biological parameters, but rather a biologically interpretable critical regime. From a biological point of view, the parameters b, h, and n are related to the energetic balance of the predator. The parameter b describes the contribution of consumed prey to predator growth, while h is related to the handling time and limits the amount of prey that a predator can consume. Then, the ratio b/h can be interpreted as the maximum asymptotic contribution of prey consumption to predator growth. The parameter n, on the other hand, represents predator

mortality. Consequently, even when prey are very abundant, predator growth may remain limited because consumption saturates and because predators face mortality and metabolic costs. This may be interpreted as a marginal energetic regime in which predation alone is not sufficient to produce positive predator growth and immigration may therefore play an important role in predator persistence. Indeed, in the absence of predator immigration, the predator per capita growth rate is

$$\frac{1}{y}\,\dot{y} = \frac{bx}{1+hx} - n.$$

Since the Holling type II functional response saturates as prey abundance increases, we have

$$\lim_{x\to\infty}\left(\frac{bx}{1+hx} - n\right) = \frac{b}{h} - n.$$

Therefore, $b > hn$ allows positive predator per capita growth for sufficiently large prey abundance, whereas for $b < hn$ predator mortality cannot be compensated by predation, even when prey are abundant. The condition $b = hn$ is precisely the critical boundary between these two regimes, under which

$$\frac{bx}{1+hx} - n = -\frac{n}{1+hx} < 0.$$

This per capita growth rate tends to zero when x tends to infinity. The biological mechanisms underlying this interpretation are well established. In particular, empirical Holling type II functional responses show that prey consumption approaches a finite maximum at high prey densities because of handling-time limitations [30]. Moreover, metabolic costs associated with foraging may substantially affect the net energetic benefit obtained by predators and, consequently, their population dynamics and persistence [16]. Thresholds obtained by comparing the maximum predation-supported growth rate with predator mortality are also standard in Rosenzweig–MacArthur and related predator–prey models [17]. The comparison between b/h and n is consistent with the bioenergetic approach to consumer-resource dynamics, in which the maximum ingestion rate is compared with the metabolic requirements of the consumer [2].

Thus, although $b = hn$ has not been empirically established for a particular predator–prey system, it represents a biologically meaningful critical regime in which immigration may become decisive for predator persistence.

In this critical regime, immigration becomes a key ecological mechanism. Since the predator population cannot sustain itself only through predation, even in the presence of abundant prey, the arrival of individuals given by the immigration term may therefore play a decisive role in maintaining the predator population and determining its long-term abundance. This highlights the importance of considering open systems when modeling ecological interactions, as immigration can qualitatively alter the system dynamics, for instance by stabilizing equilibria or enabling the emergence of oscillatory behavior that would not be observed in closed systems.

We therefore study system (1.1) with $h \neq 0$, $\alpha = 0$ and $b = hn$, representing a Holling type II functional response:

$$\begin{aligned} \dot{x} &= rx - \frac{axy}{1+hx} + c_1, \\ \dot{y} &= \frac{hnxy}{1+hx} - ny + c_2. \end{aligned} \tag{1.2}$$

We can work with an equivalent polynomial system, which allows us to use the Poincaré compactification. To obtain the equivalent system we do a time rescaling introducing the new time variable $\tau = t/(1+hx)$. Then, denoting now $\dot{x} = dx/d\tau$ and $\dot{y} = dy/d\tau$, we obtain the polynomial system:

$$\begin{aligned} \dot{x} &= rhx^2 - axy + (c_1h + r)x + c_1, \\ \dot{y} &= c_2hx - ny + c_2. \end{aligned} \tag{1.3}$$

Let us consider

$$\begin{aligned} K &= a^2c_2^2 + ac_2n(n-2r) - n^2r(c_1h + n - r), \\ T &= K^2 - 4n^2(ac_2 - nr)^2(ac_2 - nr + c_1hn). \end{aligned}$$

Our main results are the following:

Theorem 1.1. *System (1.3) admits the global phase portraits shown in Figure 1.1 in the positive quadrant of the Poincaré disk. More precisely, if $ac_2 \leq nr$, then system (1.3) has a global phase portrait topologically equivalent to the global phase portrait in Figure 1.1(A).*

If $ac_2 > nr$, $T > 0$ and $K > \sqrt{T}$ or if $T < 0$ and $K > 0$, then system (1.3) can have a global phase portrait topologically equivalent to the global phase portrait in Figure 1.1(B) or (C). If $ac_2 > nr$, $T > 0$ and $K < -\sqrt{T}$ or if $T < 0$ and $K < 0$, then system (1.3) can have a global phase portrait topologically equivalent to the global phase portrait in Figure 1.1(D) or (E).

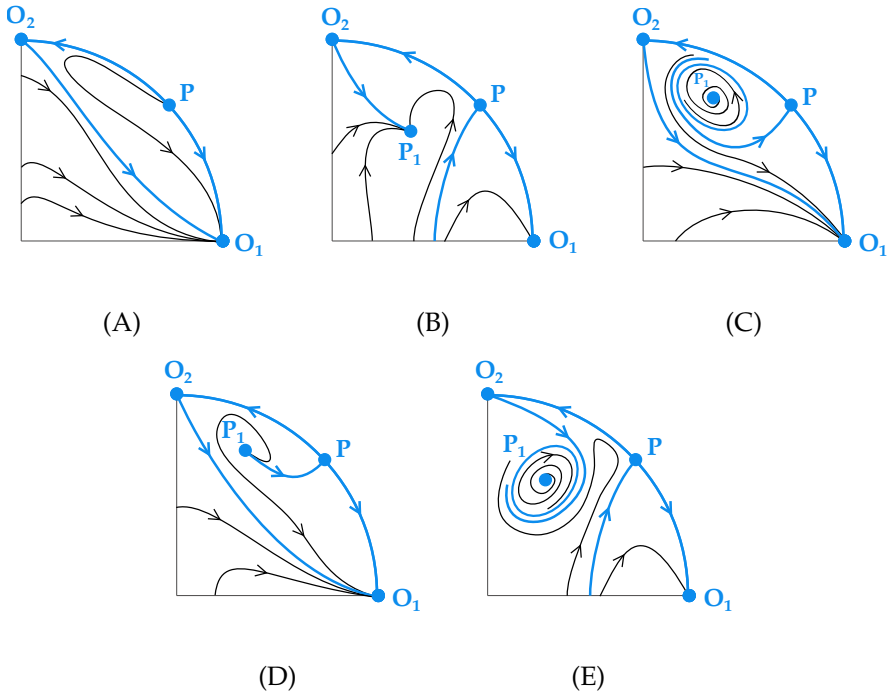


Figure 1.1: Phase portraits of system (1.3) in the positive quadrant of the Poincaré disk.

Observation 1.2. We have proved analytically that the phase portrait in Figure 1.1(A) is realizable.

For the case $ac_2 > nr$, although the existence of additional limit cycles generated through mechanisms other than the Hopf bifurcation analyzed in this paper cannot be ruled out analytically, extensive numerical simulations performed with the software *P4* did not detect any phase portrait configuration different from those shown in Figure 1.1.

If the existence of limit cycles arising through mechanisms other than the Hopf bifurcation could be ruled out, then all phase portraits shown in Figure 1.1 would be analytically justified (and no other phase portraits would be possible). Indeed, for each parameter regime considered, the local dynamics together with the configuration of the infinite equilibria determines a unique possible global arrangement of separatrices in the Poincaré disk.

Additionally, using the software *P4*, we provided numerical evidence that the phase portraits shown in Figure 1.1(B) and (D) are realizable.

The software *P4* is a numerical package designed for the qualitative study of planar polynomial differential systems. For a given set of parameters, it computes finite and infinite equilibrium points, analyzes their local phase portraits, determines separatrices, and provides a complete numerical visualization of the global phase portrait. In addition, it can search for limit cycles in prescribed regions. Further information about P4 can be found in [13, Chapter 4] and [6].

Theorem 1.3. *System (1.3) has the positive equilibrium point P_1 when $ac_2 > nr$, and this equilibrium point undergoes a Hopf bifurcation at $\tilde{c}_1 = (ac_2 - nr)(ac_2 + n(n-r))/(hn^2 r)$ when $T < 0$ and $ac_2 \neq 2nr$, for $|c_1 - \tilde{c}_1|$ sufficiently small.*

More precisely, the bifurcation is supercritical if $ac_2 - 2nr > 0$ and then for $c_1 > \tilde{c}_1$ the system has a unique small-amplitude stable limit cycle bifurcating from the equilibrium point P_1. The bifurcation is subcritical if $ac_2 - 2nr < 0$ and then for $c_1 < \tilde{c}_1$ the system has a unique small-amplitude unstable limit cycle bifurcating from the equilibrium point P_1.

The proofs of these results are organized as follows: In Section 2 we study the local dynamics at the finite equilibrium points; in Section 3 we study the dynamics at infinity by means of the Poincaré compactification. In Section 4 we analyze the existence of a Hopf bifurcation and we give sufficient conditions for it to appear, giving rise to a limit cycle. Finally, in Section 5 we study the realizable global phase portraits in the positive quadrant of the Poincaré disk.

2 Finite equilibrium points

Depending on the values of the parameters, we distinguish the following cases according to the existence of finite equilibrium points of system (1.3): If $b = hn$ and $ac_2 = nr$, the only equilibrium point is $P_0 = \left(-\frac{1}{h}, 0\right)$; If $b = hn$ and $ac_2 \neq nr$, the equilibrium points are

$$P_0 = \left(-\frac{1}{h}, 0\right) \quad \text{and} \quad P_1 = \left(\frac{c_1 n}{ac_2 - nr}, c_2\left(\frac{1}{n} + \frac{c_1 h}{ac_2 - nr}\right)\right).$$

As we are studying a population model, we are interested in studying the positive quadrant, so now we analyze when these equilibrium points are in that quadrant and which are the phase portraits in those cases. First, it is clear that the equilibrium point P_0 is always on the negative part of the x-axis, so we do not need to study it. The equilibrium point P_1 is in the positive quadrant if and only if $ac_2 > nr$, so we study its local dynamics under this condition. Let us consider K and T as previously defined.

The Jacobian matrix of system (1.3) at the equilibrium point P_1 has eigenvalues $(K \pm \sqrt{T})/(-2n(ac_2 - nr))$. The determinant is $ac_2 - nr + c_1hn > 0$, so P_1 is non-degenerate. If $T \geq 0$, then P_1 is a node: if $K > \sqrt{T}$, it is a stable node and if $K < -\sqrt{T}$ it is an unstable node; if $T < 0$ and $K > 0$, then P_1 is a stable focus and if $T < 0$ and $K < 0$, then P_1 is an unstable focus. If $K = 0$, then necessarily $T < 0$ and P_1 has a pair of purely imaginary eigenvalues; this case corresponds to $c_1 = \tilde{c}_1$ and it is studied in Section 4.

3 Dynamics at infinity

To achieve a comprehensive understanding of the behavior of system (1.3), we use the Poincaré compactification. This technique allows us to control the dynamics of a polynomial differential system near infinity. We provide a basic introduction to this method here, with more in-depth details available in Chapter 5 of [13].

The basic idea of this method consists of projecting the system from the plane onto a sphere, particularly the sphere $\mathbb{S}^2 = \{y \in \mathbb{R}^3 : y_1^2 + y_2^2 + y_3^2 = 1\}$, which is called the *Poincaré sphere*. We consider a planar polynomial system of the form

$$\dot{x_1} = P(x_1, x_2),$$
$$\dot{x_2} = Q(x_1, x_2),$$

and project it onto the sphere, obtaining induced vector fields, one in each open hemisphere of $\mathbb{S}^2$. The plane $\mathbb{R}^2$ can be identified with the tangent plane to the sphere at the point $(0, 0, 1)$. The projection can be done with the central projections $f^+ : \mathbb{R}^2 \to \mathbb{S}^2$ and $f^- : \mathbb{R}^2 \to \mathbb{S}^2$, defined by

$$f^+(x) = \left(\frac{x_1}{\Delta(x)}, \frac{x_2}{\Delta(x)}, \frac{1}{\Delta(x)}\right) \quad \text{and} \quad f^-(x) = \left(\frac{-x_1}{\Delta(x)}, \frac{-x_2}{\Delta(x)}, \frac{-1}{\Delta(x)}\right),$$

where $\Delta(x) = \sqrt{x_1^2 + x_2^2 + 1}$.

The differential Df^+ (resp. Df^-) provides a vector field in the northern (resp. southern) hemisphere, and we can extend analytically this vector field to the points of the equator multiplying the field by y_3^{d-1}, where d is the degree of the original vector field in the plane.

As the points of the equator $\mathbb{S}^1$ of $\mathbb{S}^2$ correspond to the points at infinity of $\mathbb{R}^2$, with this extension we can study the dynamics at the infinite equilibrium points, which are those in the equator of the sphere.

We consider the local charts (U_i, ϕ_i) and (V_i, ψ_i) of the sphere $\mathbb{S}^2$, where $U_i = \{y \in \mathbb{S}^2 : y_i > 0\}$, $V_i = \{y \in \mathbb{S}^2 : y_i < 0\}$, $\phi_i : U_i \longrightarrow \mathbb{R}^2$ and $\psi_i : V_i \longrightarrow \mathbb{R}^2$ for $i = 1, 2, 3$ with $\phi_i(y) = \psi_i(y) = (y_m/y_i, y_n/y_i)$ for $m < n$ and $m, n \neq i$.

The extended field, the so-called *Poincaré compactification* of the original vector field, has the following expression in the local chart (U_1, ϕ_1):

$$\dot{u} = v^d \left[-u\, P\left(\frac{1}{v}, \frac{u}{v}\right) + Q\left(\frac{1}{v}, \frac{u}{v}\right)\right], \qquad \dot{v} = -v^{d+1}\, P\left(\frac{1}{v}, \frac{u}{v}\right), \tag{3.1}$$

in the local chart (U_2, ϕ_2) the expression is

$$\dot{u} = v^d \left[P\left(\frac{u}{v}, \frac{1}{v}\right) - uQ\left(\frac{u}{v}, \frac{1}{v}\right)\right], \qquad \dot{v} = -v^{d+1}\, Q\left(\frac{u}{v}, \frac{1}{v}\right), \tag{3.2}$$

and in the local chart (U_3, ϕ_3) is

$$\dot{u} = P(u,v), \qquad \dot{v} = Q(u,v). \tag{3.3}$$

In the charts (V_i, ψ_i), with $i = 1,2,3$, the system is the same as in the charts (U_i, ϕ_i) multiplied by $(-1)^{d-1}$.

If a point $y \in \mathbb{S}^1$ is an infinite equilibrium point, then $-y$ is also an infinite equilibrium point and they have the same or opposite stability depending on whether the system has odd or even degree. Taking this into account, it is sufficient to study the infinite points on the local chart U_1 and the origin of the local chart U_2.

As we are studying a real population problem, we are only interested in the positive values of the variables, and we present the phase portraits of the polynomial differential system in the positive quadrant of the *Poincaré disk*, which is the orthogonal projection of the northern hemisphere of $\mathbb{S}^2$ onto the plane $y_3 = 0$.

In chart U_1 system (1.3) has the expression

$$\begin{aligned} \dot{u} &= -c_1 u v^2 + a u^2 - (c_1 h + n + r) u v + c_2 v^2 - h r u + c_2 h v, \\ \dot{v} &= -c_1 v^3 + a u v - (c_1 h + r) v^2 - h r v \end{aligned} \tag{3.4}$$

The equilibrium points over $v = 0$ are the origin of the local chart U_1, hereafter denoted by O_1, and the point $P = (hr/a, 0)$. We study their local behavior. First, the origin of system (3.4), i.e., the origin of chart U_1 is a hyperbolic stable node if $r > 0$, as the Jacobian matrix at this equilibrium point has an eigenvalue $-hr$ with multiplicity two. The equilibrium point $P = (hr/a, 0)$ is semi-hyperbolic: if $nr \neq ac_2$, it is a saddle-node and if $nr = ac_2$, it is an unstable node. This can be deduced by Theorem 2.19 in [13] as follows: We translate P to the origin by doing the variable change $(u, v) \to \left(U + \frac{hr}{a}, V\right)$, and we obtain the system:

$$\begin{aligned} \dot{U} = & -c_1 U V^2 + a U^2 - (c_1 h + n + r) U V + \frac{c_2 a - c_1 h r}{a} V^2 \\ & + h r U + \frac{a c_2 h + h n (c_1 h + n + r) - h (n + r)(c_1 h + n + r)}{a} V, \\ \dot{V} = & -c_1 V^3 + a U V - (c_1 h + r) V^2. \end{aligned}$$

Now we write the system in coordinates that put its linear part into Jordan normal form, by doing the variable change $(U, V) \to \left(p + (\frac{c_1 h + n + r}{a} - \frac{c_2}{r}) q, q\right)$. Thus, we obtain the system:

$$\begin{aligned} \dot{p} &= -c_1 p q^2 + a p^2 - \frac{a c_2}{r} p q + (n + r) \left(\frac{c_2}{r} - \frac{c_1 h + n}{a} \right) q^2 + h r p, \\ \dot{q} &= -c_1 q^3 + \left(n - \frac{a c_2}{r} \right) q^2 + a p q. \end{aligned}$$

We obtain the function

$$g(q) = \left(n - \frac{a c_2}{r} \right) q^2 + \left(\frac{(n + r)(r(c_1 h + n) - a c_2)}{h r^2} - c_1 \right) q^3 + o(q^3),$$

that corresponds to the dynamics on the center manifold associated with the zero eigenvalue of P. Therefore, the local phase portrait of P can be determined by applying the mentioned Theorem 2.19, in [13], by studying the first non-vanishing term in the expression of $g(q)$. We get that, if $ac_2 \neq nr$, the coefficient of degree two is non-zero, and the equilibrium point P is a saddle-node, as the degree is even. In the case $ac_2 = nr$, the coefficient of degree three

becomes $(ac_1c_2)/r^2$, which is positive, so in that case the equilibrium point is an unstable topological node.

In chart U_2 system (1.3) is written

$$\begin{aligned}\dot{u} &= -c_2hu^2v - c_2uv^2 + hru^2 + (c_1h + n + r)uv + c_1v^2 - au,\\ \dot{v} &= -c_2huv^2 - c_2v^3 + nv^2.\end{aligned}$$

The origin of this local chart, which is the only infinite equilibrium point we have to consider here, is semi-hyperbolic. Hereafter we denote this equilibrium point by O_2. The system has its linear part in Jordan normal form, but since the non-zero eigenvalue, $-a$, is negative, we change the sign of the field. We get $g(v) = -nv^2 + o(v^2)$, so the origin is a saddle-node.

4 Proof of Theorem 1.3

Let us consider $ac_2 > nr$, so the equilibrium point P_1 is on the positive quadrant. The Jacobian matrix of system (1.3) at the equilibrium point P_1 is

$$A(c_1) = \begin{pmatrix} \dfrac{c_1hnr}{ac_2 - nr} - \dfrac{ac_2}{n} + r & \dfrac{ac_1n}{nr - ac_2} \\ c_2h & -n \end{pmatrix}.$$

Assume that $T < 0$. Then the matrix $A(c_1)$ has eigenvalues $\mu(c_1) \pm \omega(c_1)i$, where

$$\mu(c_1) = \frac{a^2c_2^2 + ac_2n(n-2r) - n^2r(c_1h + n - r)}{-2n(ac_2 - nr)} \quad 0\text{and} \tag{4.1}$$

$$\omega(c_1) = \frac{\sqrt{-T}}{2n(ac_2 - nr)}. \tag{4.2}$$

We get $\mu(\tilde{c}_1) = 0$ for

$$\tilde{c}_1 = (ac_2 - nr)(ac_2 + n(n-r))/(hn^2r). \tag{4.3}$$

Therefore at $c_1 = \tilde{c}_1$ the equilibrium point P_1 has a pair of pure imaginary eigenvalues $\pm i\omega(\tilde{c}_1)$. The system will have a Hopf bifurcation if some Lyapunov constant is nonzero and $(d\mu/dc_1)(\tilde{c}_1) \neq 0$. In order to analyze this Hopf bifurcation, we apply [20, Theorem 3.3], and for that we must check whether the genericity conditions are satisfied. We check that the transversality condition is satisfied as

$$\frac{d\mu}{dc_1}(\tilde{c}_1) = \frac{hnr}{2(ac_2 - nr) > 0.} \tag{4.4}$$

To check the second condition, we must compute the first Lyapunov constant. We fix the value $c_1 = \tilde{c}_1$ and then the equilibrium P_1 has the expression

$$P_1 = \left(\frac{ac_2 + n^2 - nr}{hnr}, \frac{c_2(ac_2 + n^2)}{n^2r}\right). \tag{4.5}$$

We translate P_1 to the origin of coordinates obtaining the system

$$\begin{aligned}\dot{\varepsilon}_1 &= hr\varepsilon_1^2 - a\varepsilon_1\varepsilon_2 + n\varepsilon_1 + \frac{anr - a^2c_2 - an^2}{hnr}\varepsilon_2,\\ \dot{\varepsilon_2} &= c_2h\varepsilon_1 - n\varepsilon_2,\end{aligned} \tag{4.6}$$

which can be represented as

$$\dot{\varepsilon} = A\varepsilon + \frac{1}{2}B(\varepsilon,\varepsilon) + \frac{1}{6}C(\varepsilon,\varepsilon,\varepsilon), \tag{4.7}$$

where $A = A(\tilde{c}_1)$ and the multilinear functions B and C are given by

$$B(\varepsilon,\eta) = \begin{pmatrix} 2hr\varepsilon_1\eta_1 - a\varepsilon_1\eta_2 - a\varepsilon_2\eta_1 \\ 0 \end{pmatrix},$$

$$C(\varepsilon,\eta,\zeta) = \begin{pmatrix} 0 \\ 0 \end{pmatrix}.$$

We compute two eigenvectors p, q of the matrix A verifying

$$Aq = i\omega q, \qquad A^T p = -i\omega p, \quad \text{and} \quad \langle p, q\rangle = 1,$$

as for example

$$q = \begin{pmatrix} \frac{1}{2}\left(1 - \frac{n}{\sqrt{\frac{(ac_2+n^2)(ac_2-nr)}{nr}}}\, i\right) \\ -\frac{c_2 h}{2\sqrt{\frac{(ac_2+n^2)(ac_2-nr)}{nr}}}\, i \end{pmatrix} \quad \text{and} \quad p = \begin{pmatrix} 1 \\ -\frac{n}{c_2 h} - \frac{\omega}{c_2 h} i \end{pmatrix}. \tag{4.8}$$

Now we compute the functions g_{20}, g_{11} and g_{21}:

$$\begin{aligned} g_{20} &= \langle p, B(q,q)\rangle \\ &= \frac{hnr\left(\sqrt{\frac{(ac_2+n^2)(ac_2-nr)}{nr}} - n\, i\right)\left(ac_2\, i + r\left(\sqrt{\frac{(ac_2+n^2)(ac_2-nr)}{nr}} - n\, i\right)\right)}{2(ac_2+n^2)(ac_2-nr)}, \\ g_{11} &= \langle p, B(q,\overline{q})\rangle = \frac{ac_2 hr}{2ac_2+2n^2}, \quad g_{21} = \langle p, C(q,q,\overline{q})\rangle = 0. \end{aligned}$$

Then, the first Lyapunov coefficient is

$$\ell_1 = \frac{1}{2\omega^2}\mathrm{Re}(ig_{20}g_{11} + \omega g_{21}) = \frac{-ac_2 h^2 nr^2(ac_2 - 2nr)}{8(ac_2+n^2)^2(ac_2-nr)\sqrt{\frac{(ac_2+n^2)(ac_2-nr)}{nr}}}.$$

Then, if $ac_2 \neq 2nr$, the first Lyapunov coefficient is non-zero, and so the second condition of the theorem we are applying is satisfied, and the equilibrium point P_1 undergoes a Hopf bifurcation. More precisely, if $ac_2 - 2nr > 0$, the bifurcation is supercritical and a unique stable limit cycle bifurcates from the equilibrium point P_1 for $c_1 > \tilde{c}_1$ with $c_1 - \tilde{c}_1$ sufficiently small; if $ac_2 - 2nr < 0$, the bifurcation is subcritical and a unique unstable limit cycle bifurcates from the equilibrium point P_1 for $c_1 < \tilde{c}_1$ with $\tilde{c}_1 - c_1$ sufficiently small.

5 Global dynamics

In this section we study the compatibility of finite and infinite equilibrium points, analyzing the possible connections between separatrices and the configurations that arise in each case. We will consider the phase portraits in the positive quadrant of the Poincaré disk, as it is the region with biological meaning. Furthermore, this is consistent as the positive quadrant is positively invariant because the flow over the positive vertical and horizontal semi-axes points towards the interior of the region.

5.1 Case $ac_2 = nr$

In this case the only finite equilibrium point is P_0, which is not in the positive quadrant of the Poincaré disk. The flow enters the region of the positive quadrant over the x- and y-axes. As there is no finite equilibrium point inside this region, there cannot be periodic orbits.

Regarding the infinite equilibrium points, the origin of chart U_1 is a stable node and the equilibrium point P on U_1 is on the boundary of the positive quadrant and it is an unstable node as $ac_2 = nr$. Finally, the origin of chart U_2 is a saddle-node.

Studying the flow over the y-axis we determine that for y large enough (more precisely for $y > c_2/n$) the flow points downwards, and this only allows one configuration for the saddle-node in the origin of chart U_2, which must have a separatrix that leaves the equilibrium point and enters in the positive quadrant. Then there is only one possible global configuration for the orbits, which is given in Figure 1.1(A).

5.2 Case $ac_2 \neq nr$

In this case there are two equilibrium points, P_0, which is never in the positive quadrant, and P_1, whose position depends on the parameters.

If $ac_2 < nr$, then P_1 is not in the positive quadrant. The origin of chart U_1 is a stable node, and the point P is now a saddle-node as $nr \neq ac_2$. The origin of chart U_2 is again a saddle-node, and the position of its separatrices is the same as in the previous case. At the equilibrium point P, the flow over the boundary of the disk is determined by the eigenvalue $hr > 0$, and there is only one possible position for the separatrix: if the separatrix goes from the finite region to the equilibrium point P starting at the origin of chart U_2, then a canonical region with periodic orbits would appear, but this is not possible as those periodic orbits should enclose an equilibrium point which does not exist. If the separatrix goes from the x-axis or the y-axis to the equilibrium point P, then the separatrix leaving from the origin of U_2 has no possible ω-limit, so this situation is not feasible. Then the only feasible position for the sectors and the separatrix of the infinite equilibrium point P is the one in which the hyperbolic sectors are outside the positive quadrant of the Poincaré disk, and the parabolic sector is inside the disk, so finally, although the local phase portrait of P is different from the previous case, by considering only the positive quadrant we obtain the same global phase portrait as in Figure 1.1(A).

If $ac_2 > nr$, then P_1 is in the positive quadrant, and it can be a node or a focus. For the other equilibrium points in the positive quadrant, we have that the origin of U_1 is a stable node, the origin of chart U_2 has two hyperbolic sectors and the separatrix between them starts at that point and goes into the positive region, and there is a separatrix that goes to the point P, separating the two hyperbolic sectors of that point. Below we analyze the different possibilities depending on the phase portrait at P_1.

- If $T > 0$ and $K > \sqrt{T}$ or if $T < 0$ and $K > 0$, then P_1 is a stable node or a stable focus, which are topologically equivalent. For this case, Figures 1.1(B) and (C) provide realizable phase portraits in the positive quadrant of the Poincaré disk.

  We have used the software P4 to provide numerical evidence that phase portrait (B) is realizable. In particular, for $K > \sqrt{T}$ phase portrait (B) can be obtained for the values $b = r = a = n = h = 1$, $c_1 = 3/256$ and $c_2 = 3/2$, and for $T < 0$ and $K > 0$, phase portrait (B) can be obtained for $b = a = c_1 = c_2 = n = h = 1$ and $r = 1/2$.

In the case $T < 0$ and $K > 0$, as we have $K = hn^2r(\tilde{c}_1 - c_1)$, then $c_1 < \tilde{c}_1$. Consequently, if $ac_2 - 2nr < 0$, Theorem 1.3 guarantees the existence of a unique small-amplitude unstable limit cycle bifurcating from P_1. Combining this local configuration with the information on the infinite equilibrium points yields the realizable phase portrait in Figure 1.1(C).

If $ac_2 - 2nr > 0$ the bifurcation is supercritical and the limit cycle exists only for $c_1 > \tilde{c}_1$, so it does not appear in this case.

- If $T > 0$ and $K < -\sqrt{T}$ or if $T < 0$ and $K < 0$, then P_1 is an unstable node or an unstable focus, which are topologically equivalent. Figures 1.1(D) and (E) provide realizable phase portraits in the positive quadrant of the Poincaré disk.

  We have used the software P4 to provide numerical evidence that phase portrait (D) is realizable. In particular, for $K < -\sqrt{T}$ phase portrait (D) can be obtained for the values $b = r = a = n = h = 1$, $c_1 = 4$ and $c_2 = 3/2$, and for $T < 0$ and $K < 0$, phase portrait (D) can be obtained for $b = a = c_2 = n = h = 1$, $r = 1/2$ and $c_1 = 2$.

  In the case $T < 0$ and $K < 0$, as we have $K = hn^2r(\tilde{c}_1 - c_1)$, then $\tilde{c}_1 < c_1$. Consequently, if $ac_2 - 2nr > 0$, Theorem 1.3 guarantees the existence of a unique small-amplitude stable limit cycle bifurcating from P_1. Combining this local configuration with the information on the infinite equilibrium points yields the realizable phase portrait in Figure 1.1(E).

6 Conclusions

In this work, we have analyzed a predator–prey system with Holling type II functional response under a critical regime for the predator, incorporating immigration in both species. This framework extends previous models (such as [10]) by combining a more realistic functional response with a regime in which the predator operates under marginal energetic conditions.

Compared with the results obtained in [10] for the Holling type I functional response, the Holling type II response considered here leads to richer dynamical behavior. In particular, the positive equilibrium may fail to exist or may change its stability, and Hopf bifurcations may occur, giving rise to small-amplitude limit cycles that can be either stable or unstable. This highlights the significant effect of consumption saturation on the global behavior of predator–prey systems.

Furthermore, in cases where the positive equilibrium point is stable, it is not globally asymptotically stable. Indeed, the existence of basin boundaries implies that different initial conditions may lead to qualitatively different long-term behaviors. In particular, trajectories outside the basin of attraction of the positive equilibrium should not be interpreted as corresponding to predator extinction, since predator immigration is always present. Rather, they may evolve towards regimes where the predator population remains at low density despite the continuous arrival of individuals through immigration.

Our main contribution is the analysis of the dynamics in the biologically relevant region, namely the positive quadrant of the Poincaré disk. By means of the Poincaré compactification, we described the local behavior at the finite and infinite equilibrium points and studied the compatibility of their separatrices. This analysis allowed us to identify the phase portrait configurations shown in Figure 1.1. The realizability of the phase portrait corresponding to

$ac_2 \leq nr$ was proved analytically, while numerical computations performed with P4 provided parameter values realizing the configurations without limit cycles when $ac_2 > nr$. Although our numerical exploration did not reveal any additional configurations, the possible existence of further limit cycles arising through mechanisms other than the Hopf bifurcation considered here cannot be ruled out analytically. If the non-existence of such additional limit cycles were established, Theorem 1.1 would yield a complete topological classification of the global phase portraits of system (1.3) in the positive quadrant of the Poincaré disk.

From an ecological perspective, the phase portraits in Figure 1.1 illustrate different possible long-term outcomes depending on the parameter values and initial population sizes. The basin boundaries separate initial conditions leading to different asymptotic behaviors, while the limit cycles arising through Hopf bifurcation represent sustained oscillations in prey and predator abundance. In particular, a small-amplitude unstable limit cycle locally separates trajectories exhibiting different behaviors near the positive equilibrium, showing that relatively small differences in the initial population sizes may produce qualitatively different population dynamics. Moreover, trajectories approaching infinity represent unbounded population growth within the mathematical model. Such behavior should not be interpreted as a realistic long-term ecological prediction, but rather as an indication that, in these regimes, the mechanisms included in the model are not sufficient to regulate population growth. In a real ecosystem, additional density-dependent effects, such as resource limitation, intraspecific competition, environmental carrying capacity, or changes in predation pressure, would be expected to prevent indefinite growth. Thus, these trajectories also help identify parameter regimes in which additional ecological mechanisms should be incorporated into the model.

In addition, we established explicit conditions for the existence of a Hopf bifurcation at the positive equilibrium. Depending on the parameter values, this bifurcation gives rise to either a stable or an unstable small-amplitude limit cycle, showing that oscillatory dynamics may occur in the presence of immigration even when the predator population is close to its survival threshold.

These findings highlight the significant role of immigration in ecological modeling, as it can affect the behavior of the system, particularly in terms of stability and the emergence of periodic orbits. From an applied perspective, this work provides a more biologically realistic framework for understanding predator–prey interactions in open ecosystems.

Future work could address more general forms of immigration (e.g., density-dependent or time-dependent terms), as well as the extension of these techniques to higher-dimensional models or to systems with additional ecological mechanisms such as delays.

Acknowledgements

The authors are partially supported by the Consellería de Educación, Universidade e Formación Profesional (Xunta de Galicia), Grant ED431C 2023/31 with FEDER funds.

References

[1] M. A. Abbasi, Fixed points stability, bifurcation analysis, and chaos control of a Lotka–Volterra model with two predators and their prey, *Int. J. Biomath.* **17**(2024), No. 4, 2350032. https://doi.org/10.1142/S1793524523500328

[2] P. A. Abrams, L. R. Ginzburg, The nature of predation: prey dependent, ratio dependent or neither?, *Trends Ecol. Evol.* **15**(2000), No. 8, 337–341. https://doi.org/10.1016/S0169-5347(00)01908-X

[3] I. Al-Darabsah, X. Tang, Y. Yuan, A prey–predator model with migrations and delays, *Discrete Contin. Dyn. Syst. Ser. B* **21**(2016), No. 3, 737–761. https://doi.org/10.3934/dcdsb.2016.21.737

[4] Z. Ali, F. Rabiei, K. Hosseini, A fractal-fractional-order modified predator–prey mathematical model with immigrations, *Math. Comput. Simul.* **207**(2023), 466–481. https://doi.org/10.1016/j.matcom.2023.01.006

[5] S. Apima, A predator–prey model with logistic growth for constant delayed migration, *J. Adv. Math. Comput. Sci.* **35**(2020), No. 3, 51–61. https://doi.org/10.9734/jamcs/2020/v35i330259

[6] J. C. Artés, F. Dumortier, C. Herssens, J. Llibre, P. De Maesschalck, Computer program P4 to study phase portraits of planar polynomial differential equations, 2005. http://mat.uab.es/~artes/p4/p4.htm [Online; accessed September 15, 2026].

[7] D. Cammarota, N. Z. Monteiro, R. Menezes, H. Fort, A. M. Segura, Lotka–Volterra model with Allee effect: equilibria, coexistence and size scaling of maximum and minimum abundance, *J. Math. Biol.* **87**(2023), No. 6, 82. https://doi.org/10.1007/s00285-023-02012-5

[8] Y. Chen, F. Zhang, Dynamics of a delayed predator–prey model with predator migration, *Appl. Math. Model.* **37**(2013), 1400–1412. https://doi.org/10.1016/j.apm.2012.04.012

[9] S. N. Chowdhury, J. Banerjee, M. Perc, D. Ghosh, Eco-evolutionary cyclic dominance among predators, prey, and parasites, *J. Theor. Biol.* **564**(2023), 111446. https://doi.org/10.1016/j.jtbi.2023.111446

[10] É. Diz-Pita, Global dynamics of a predator–prey system with immigration in both species, *Electron. Res. Arch.* **32**(2024), No. 2, 762–778. https://doi.org/10.3934/era.2024036

[11] É. Diz-Pita, M. V. Otero-Espinar, Predator–prey models: a review of some recent advances, *Mathematics* **9**(2021), No. 15, 1783. https://doi.org/10.3390/math9151783

[12] É. Diz-Pita, J. Llibre, M. V. Otero-Espinar, Global phase portraits of a predator–prey system, *Electron. J. Qual. Theory Differ. Equ.* **2022**, No. 16, 1–13. https://doi.org/10.14232/ejqtde.2022.1.16

[13] F. Dumortier, J. Llibre, J. C. Artés, *Qualitative theory of planar differential systems*, Universitext, Springer-Verlag, Berlin, Heidelberg, 2006. https://doi.org/10.1007/978-3-540-32902-2

[14] C. Egevang, I. J. Stenhouse, R. A. Phillips, A. Petersen, J. W. Fox, J. R. D. Silk, Tracking of Arctic terns *Sterna paradisaea* reveals longest animal migration, *Proc. Natl. Acad. Sci. USA* **107**(2010), No. 5, 2078–2081. https://doi.org/10.1073/pnas.0909493107

[15] Z. Eskandari, P. A. Naik, M. Yavuz, Dynamical behaviors of a discrete-time prey–predator model with harvesting effect on the predator, *J. Appl. Anal. Comput.* **14**(2024), No. 1, 283–297. https://doi.org/10.11948/20230212

[16] H. C. Giacomini, Metabolic responses of predators to prey density, *Front. Ecol. Evol.* **10**(2022), 980812. https://doi.org/10.3389/fevo.2022.980812

[17] A. Hammoum, T. Sari, K. Yadi, The Rosenzweig–MacArthur graphical criterion for a predator–prey model with variable mortality rate, *Qual. Theory Dyn. Syst.* **22**(2023), Art. No. 36. https://doi.org/10.1007/s12346-023-00739-6

[18] B. Hoare, *Animal migration: remarkable journeys by air, land and sea*, Natural History Museum, London, United Kingdom, 2009.

[19] F. Kangalgil, S. Isik, Effect of immigration in a predator–prey system: stability, bifurcation and chaos, *AIMS Math.* **7**(2022), No. 8, 14354–14375. https://doi.org/10.3934/math.2022791

[20] Y. A. Kuznetsov, *Elements of applied bifurcation theory*, 2nd ed., Springer-Verlag, New York, 1998. https://doi.org/10.1007/b98848

[21] J. Li, X. Liu, C. Wei, The impact of role reversal on the dynamics of predator–prey model with stage structure, *Appl. Math. Model.* **104**(2022), 339–357. https://doi.org/10.1016/j.apm.2021.11.029

[22] J. Llibre, Y. P. Mancilla-Martínez, Global attractor in the positive quadrant of the Lotka–Volterra system in $\mathbb{R}^2$, *Internat. J. Bifur. Chaos Appl. Sci. Engrg.* **33**(2023), No. 12, 2350147. https://doi.org/10.1142/S021812742350147X

[23] D. Mukherjee, The effect of refuge and immigration in a predator–prey system in the presence of a competitor for the prey, *Nonlinear Anal. Real World Appl.* **31**(2016), 277–287. https://doi.org/10.1016/j.nonrwa.2016.02.004

[24] P. A. Naik, Z. Eskandari, M. Yavuz, J. Zu, Complex dynamics of a discrete-time Bazykin–Berezovskaya prey–predator model with a strong Allee effect, *J. Comput. Appl. Math.* **413**(2022), 114401. https://doi.org/10.1016/j.cam.2022.114401

[25] P. A. Naik, Z. Eskandari, H. E. Shahkari, K. M. Owolabi, Bifurcation analysis of a discrete-time prey–predator model, *Bull. Biomath.* **1**(2023), No. 2, 111–123. https://doi.org/10.59292/bulletinbiomath.2023006

[26] M. Priyanka, P. Muthukumar, S. Bhalekar, Stability and bifurcation analysis of two-species prey–predator model incorporating external factors, *Int. J. Bifurcat. Chaos* **32**(2022), No. 11, 2250172. https://doi.org/10.1142/S0218127422501723

[27] S. M. S. Rana, Bifurcation and complex dynamics of a discrete-time predator–prey system, *Comput. Ecol. Softw.* **5**(2015), No. 2, 187–200.

[28] J. Sugie, Y. Saito, Uniqueness of limit cycles in a Rosenzweig–MacArthur model with prey immigration, *SIAM J. Appl. Math.* **72**(2012), No. 1, 299–316. https://doi.org/10.1137/11084008X

[29] T. Tahara, M. K. A. Gavina, T. Kawano, J. M. Tubay, J. F. Rabajante et al., Asymptotic stability of a modified Lotka–Volterra model with small immigrations, *Sci. Rep.* **8**(2018), 7029. https://doi.org/10.1038/s41598-018-25436-2

[30] R. N. Wiedenmann, R. J. O'Neil, Laboratory measurement of the functional response of *Podisus maculiventris* (Say) (Heteroptera: Pentatomidae), *Environ. Entomol.* **20**(1991), No. 2, 610–614. https://doi.org/10.1093/ee/20.2.610

[31] G. Zhu, J. Wei, Global stability and bifurcation analysis of a delayed predator–prey system with prey immigration, *Electron. J. Qual. Theory Differ. Equ.* **2016**, No. 13, 1–20. https://doi.org/10.14232/ejqtde.2016.1.13